Theory of the Bloch Oscillating Transistor

J. Hassel, and H. Seppä

VTT Information Technology, Microsensing,

P.O. Box 1207, FIN-02044 VTT

Abstract. The Bloch oscillating transistor (BOT) is a device, where single electron current through a normal tunnel junction enhances Cooper pair current in a mesoscopic Josephson junction leading to signal amplification. In this paper we develop a theory, where the BOT dynamics is described as a two-level system. The theory is used to predict current-voltage characteristics and small-signal response. The transition from stable operation into hysteretic regime is studied. By identifying the two-level switching noise as the main source of fluctuations, the expressions for equivalent noise sources and the noise temperature are derived. The validity of the model is tested by comparing the results with simulations and experiments.

PACS numbers: 74.78.Na, 85.25.Am, 85.35.Gv

I. INTRODUCTION

The Bloch oscillating transistor (BOT)[1−5] is based on tuning the probability of interlevel switching in a mesoscopic Josephson Junction (JJ). The equivalent circuit is shown in Fig. 1(a). The current I_C at the collector(C) -emitter(E) -circuit is controlled by the base current I_B leading to transistor-like operation. The physics is based on controlling the state of the JJ by means of quasiparticles tunneling through the normal tunnel junction connected to the base electrode (B).

The state diagram as function of the (quasi)charge Q_I is shown in Fig. 1(b)[6], where also the transitions are illustrated. It is assumed that the Josephson coupling energy E_J is smaller or of the same order as the charging energy $E_C = e^2/2C_\Sigma$, and that $R, R_{T1}, R_{T2} \gtrsim R_Q$. Here $C_\Sigma = C_1 + C_2$ is the total capacitance of the junctions, R is the collector resistor, and R_{T1} and R_{T2} are the tunnel resistances. The quantum resistance $R_Q = h/4e^2 \approx 6.5$ kΩ. We assume that C is biased at a point, where $V_C \gtrsim e/C_\Sigma$. The charge tends to relax through the collector resistor R_C towards $V_C C_\Sigma$. Here V_C is the collector voltage. If the system is initially at the lowest band ($|Q_I| < e$ in the extended band picture we are using), at $Q_I = e$ it is likely that a Cooper pair (CP) tunneling through the JJ returns the system back to $Q_I = -e$. Repeating this cycle, the Bloch Oscillation[6], leads to a net current through the

C-E circuit. We call the lowest band with allowed Cooper pair conduction the "first level".

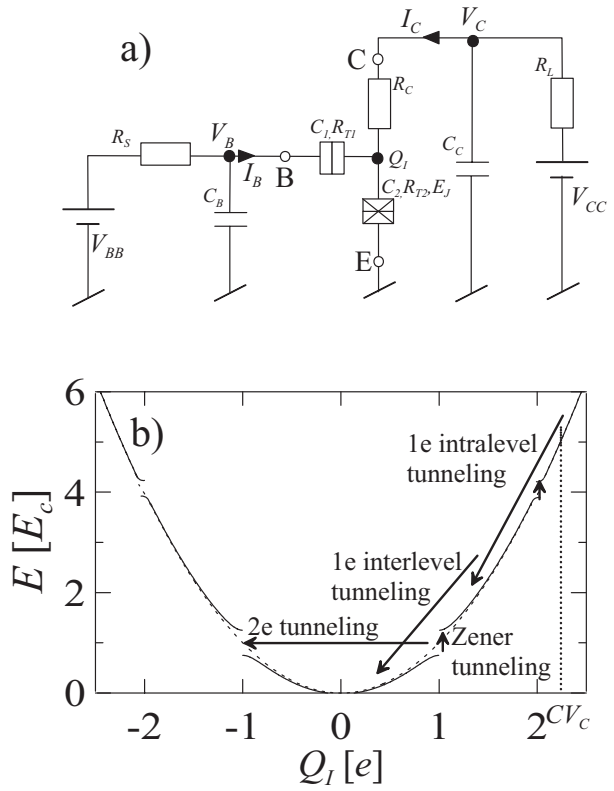

FIG. 1: *(a) Schematic circuit of a BOT connected to a source and a load. Source R_S is connected to the base electrode B and load R_L to the collector electrode C. The lead capacitances from the electrodes to the ground are C_B and C_C. The BOT itself consists of a Josephson Junction (JJ) connected to E, a normal tunnel junction connected to B and large $R_C \gg R_Q$ resistor connected to C. All three components are further connected to a superconducting node, which has small capacitance to the ground. (b) The state diagram of the JJ and the possible transitions.*

A competing process with the CP tunneling is the Zener tunneling[7], which provides a mechanism for an upwards transition. Zener tunneling takes the system to the upper bands ($|Q_I| > e$). Cooper pairs are allowed to tunnel only near the band gaps $|Q_I| = ne$, where n is an integer. However, in the limit of small E_J/E_C the Zener tunneling probability increases very rapidly as function of the band index n. Therefore CP tunneling is virtually blocked for $|Q_I| > e$. This enables us to treat the system as a two-level system. The "second level" consists of the higher bands with blocked CP tunneling. Downwards transitions are induced by one or more quasiparticles tunneling through the base junction (see Fig. 1(b)). Tuning the quasiparticle tunneling probability by changing base voltage or current leads to the control of average current through the C-E circuit, and thus to transistor-like characteristics.

The BOT was recently experimentally realized[3], and simulations showed that its properties can be quantitatively predicted with a computational model[5]. It is potentially useful in cryogenic applications such as readout circuits of radiation detectors, or measurement of small currents in quantum metrology. The aim of this article is to gain more insight into the BOT and to study the noise properties. To be able to do so, we derive an analytic theory, and study its applicability by comparing the results to computational and experimental data.

II. ANALYTIC THEORY

In the theory derived below, BOT is modelled as a mapping of voltages V_B and V_C into currents I_B and I_C. We assume that a single tunneling event will not affect the voltages. This is the case, since $C_B, C_C \gg C_\Sigma$ in a practical experimental setup.

We assume that $1 \ll E_C/kT \ll R_C/R_Q$ and $E_J \ll E_C$, which means that the Cooper pair tunneling rate reduces to a delta spike centered at $|Q_I| = e$ [8,9]. This recovers our interpretation of the two-level system. We also assume that $C_2 \gg C_1$ and neglect quasiparticle tunneling through the JJ. Below unnecessary subscripts for capacitances and charges are dropped, i.e. $C \equiv C_2 \equiv C_\Sigma$, $R \equiv R_C$, $R_T \equiv R_{T1}$ and $Q \equiv Q_I \equiv Q_2$. We analyze only the regime, where $V_C > e/C$ and $V_B' < 0$, since this is interesting for the amplifier operation. Here we have defined $V_B' = V_B - V_C$.

The collector and base currents are written as

$$I_C = \frac{1/\Gamma_\uparrow}{1/\Gamma_\uparrow + 1/\Gamma_\downarrow} I_S - I_B \tag{1}$$

$$I_B = -\frac{\langle N_e \rangle \, e}{1/\Gamma_\uparrow + 1/\Gamma_\downarrow}, \tag{2}$$

The transition rates between the two levels are $\Gamma_\uparrow$ and $\Gamma_\downarrow$. The "saturation current", i.e. current through the JJ at the first level, is $I_S = 2ef_B$, where f_B is the Bloch oscillations frequency. The number of electrons needed to induce a downwards transition is $\langle N_e \rangle$. Here we have neglected the possibility of single-electron tunneling, when the system is at the first level. This is justified, since typically the voltage $|V_1|$ is below the gap voltage in that case. The Eqs. (1) and (2) give general IV characteristics for the BOT.

Between tunneling events $dQ/dt = (V_C - Q/C)/R$. By integrating from $Q = -e$ to $Q = e$, i.e. over one Bloch period one gets f_B, and consequently

$$I_S = \frac{2V_Q}{R} \left[\ln \left(\frac{V_C/V_Q + 1}{V_C/V_Q - 1} \right) \right]^{-1}, \tag{3}$$

where we have defined $V_Q = e/C$.

The upwards tunneling rate (the Zener tunneling) can now be written as[10]

$$\Gamma_\uparrow = \frac{I_S}{2e\,\langle N\rangle}, \tag{4}$$

where

$$\langle N\rangle = \exp\left(\frac{I_z R}{V_C - V_Q}\right) - 1 \tag{5}$$

is the average number of Cooper pairs in one sequence of Bloch oscillations. One sequence here means the time between tunneling down to the first level and tunneling back to the second level. The Zener avalanche current is $I_z = \pi e E_J^2/8\hbar E_c$.

The downwards tunneling at low temperatures and for large R is exclusively due to single electron tunneling through the base junction. It is generally impossible to calculate exact analytic expressions for $\langle N_e\rangle$ and $\Gamma_\downarrow$. We proceed, however, by giving approximations in two limits. For $V_C < 2V_Q$ one electron always suffices to induce a downwards transition. Assuming further the low-temperature and large resistance limit of base electrode tunneling rates, and that the transient is short compared to the inverse of the tunneling rate, it follows[11]

$$\langle N_e\rangle = 1 \tag{6}$$

$$\Gamma_\downarrow = -\frac{1}{CR_T}\left(\frac{V_B'}{V_Q} + \frac{1}{2}\right). \tag{7}$$

If $V_C > 2V_Q$ the first electron tunneling through the base junction does not necessarily cause a transition to the first level, but some of but intralevel transitions occur instead. In this limit we have solved the problem numerically, and searched for a proper fitting function. The result is[11].

$$\langle N_e\rangle = 0.04\left(\frac{R_T}{R}\right)^2 \times \exp\left(0.3\exp\left(1.8\frac{V_C}{V_Q} + 0.27\frac{V_C V_B'}{V_Q^2} - 0.2\frac{V_B'}{V_Q}\right)\right) + 1 \tag{8}$$

$$\Gamma_\downarrow^{-1} = 1.2e\frac{R+R_T}{V_B'}\left(1 - \langle N_e\rangle\right) + RC\left(2.5\frac{R_T}{R} + 1.1\right)\left(\frac{V_Q}{V_B'}\right)^2. \tag{9}$$

The fit is accurate, when $R_T \lesssim R$. The weaker dependence indicated by the unity term in Eq. (8) and $(2.5R_T/R + 1.1)\,(V_B'/V_Q)^2$ term in Eq. (9) dominate at $V_C \approx 2V_Q$ and large $|V_B'|$. In this case only one quasiparticle is needed to induce a downwards transition. This is possible, if the tunneling occurs during the transient immediately after the Zener tunneling, while still

$Q(t) < 2e$. The $\exp(0.3\exp(...))$-term dominates, when several tunneling events are needed to induce an interlevel transition. The very strong dependence is roughly explained as follows. Let us assume that $2V_Q < V_C < 3V_Q$ and the island charge is initially $Q \approx CV_C$ (see Fig. 1). Now at least two quasiparticles tunneling rapidly one after another are needed to induce a downwards transition. The quasiparticle tunneling probability is at its maximum, when $Q \approx CV_C$. However, after the first tunneling event Q drops down to $CV_C - e$ and therefore the probability also drops. Hence the probability for the second quasiparticle to tunnel before the charge relaxes back to $Q > 2e$ is small. The charge therefore tends to oscillate between $Q \approx CV_C$ and $Q \approx CV_C - e$ for a long time before the rather improbable event at $Q < 2e$ happens. This generates a large quantity of intralevel transitions thus increases $\langle N_e \rangle$ and decreases $\Gamma_\downarrow$.

III. COMPARING NUMERIC, ANALYTIC AND EXPERIMENTAL IV CURVES

In this Section we compare the results with the numerical model[5] based on the phase-correlation theory[8,9]. Earlier, it has been found to agree well with experimental results. Thus we believe that it provides evidence on the applicability of the analytic theory, though in the limit of large R, a simpler quasiclassical theory[6] should work as well. Also a direct comparison to experimental data is performed below.

In Fig. 2(a) we show a simulated set of $I_C - V_C$ curves (open circles), where the base is voltage biased. The base voltage V_B' is varied, while other parameters are $R = 1.5$ MΩ, $C = 0.2$ fF, $R_T = 12$ MΩ, $E_J/E_C = 0.1$, $T = 40$ mK and $\Delta = 1.5$ mV. Corresponding analytic curves (solid lines) are calculated from Eq. (1) using the approximation of Eqs. (6) and (7) when calculating $\langle N_e \rangle$ and $\Gamma_\downarrow$. The agreement is reasonably good. An error is caused by the finite temperature and the superconducting energy gap, when calculating the quasiparticle tunneling rate of the base junction. If the tunneling rates are computed numerically from the phase-correlation theory, the agreement is improved especially at low values of V_B' as denoted by the dashed lines in Fig. 2(a).

The remaining disagreement is related to the temperature dependence of Cooper pair tunneling probabilities. Even if E_C/kT is as high as about 120, incoherent Cooper pair tunneling enhances Cooper pair current at $V_C \approx V_Q = 800$ μV. The lower value of simulated I_C at larger values of V_C was found to be due to the fact that after a Cooper pair tunnels through the JJ, it can immediately tunnel into the opposite direction due to incoherent Cooper pair tunneling. This effectively suppresses $\langle N \rangle$, or equivalently enhances $\Gamma_\uparrow$. The effect is especially visible in Fig. 2(b), where a set of simulations with a current biased base electrode is performed for the same device. The simulated curves (solid circles) fall below the theoretical curves (lines) $I_C = (2\langle N \rangle + 1) I_B$ (see also Section IV), i.e. the current gain is suppressed. However, if we artificially forbid the "Cooper-pair back-tunneling" in the simulation (open squares in Fig. 2(b)) the agreement is clearly improved. This shows that

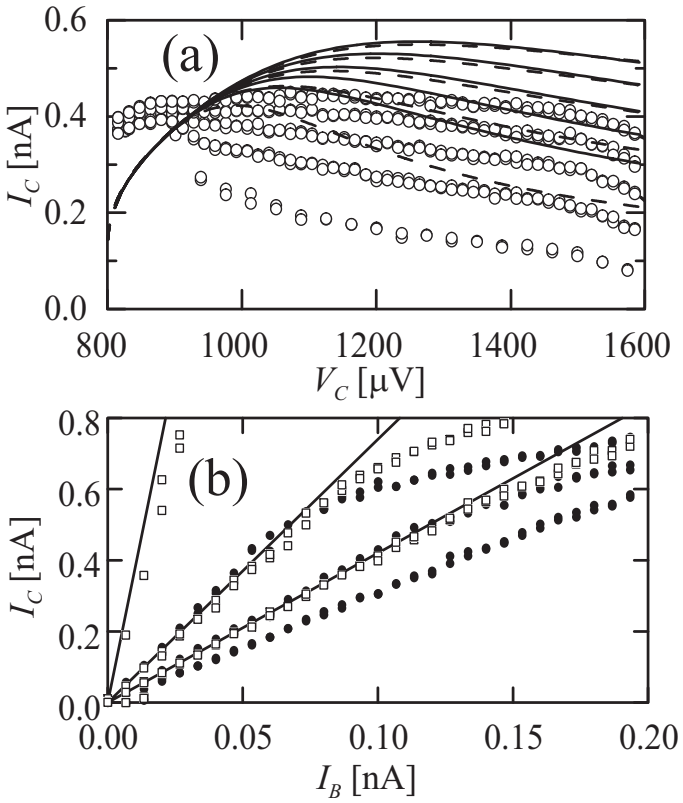

FIG. 2: *(a) Computed I_C-V_C plots with $R = 1.5$ $M\Omega$, $C = 0.2$ fF, $R_T = 12$ $M\Omega$, $E_J/E_C = 0.1$, $T =$ 40 mK and $\Delta = 1.5$ mV (open circles). The base voltage has been varied as $V_B' = -2.5e/C$, -3.0e/C, -3.5e/C, -4.0e/C, -4.5e/C from down to top. Solid lines represent analytic values calculated from Eq. (1) together with approximations from Eqs. (6) and (7). Dashed lines are corrected analytic curves, which take base junction nonlinearity at the finite temperature into account. (b) Computed I_C-I_B plots for the same device (solid circles) at V_C =1.25e/C, 1.5e/C, 1.75e/C from up to down. The open squares shows the same simulation without "Cooper pair back-tunneling" and lines show analytic predictions.*

the effect indeed is the main factor suppressing the current gain in the point of operation governed by approximation given in Eqs. (6) and (7). Another mechanism due to spontaneous downwards transitions was discussed in Ref.[4], but it was found to be insignificant in this case.

As the tunnel resistance of the base electrode is decreased and the Josephson coupling increased in simulations and experiments citedel1,[5], the active bias region moves towards higher V_C indicating that the approximation of $\langle N_e \rangle$ and $\Gamma_\downarrow$ given in Eq:s (8) and (9) becomes relevant. In Fig. 3(a) a set of simulations with parameters similar to those considered above, with exceptions $R_T = 375$ kΩ, $E_J/E_C = 0.2$ and $\Delta = 0$ for the base junction (i.e. we have assumed that the base junction is a NIN junction here). At the upper set it is again shown a

set of simulated and analytic $I_C - V_C$ curves showing a reasonable agreement. The agreement is again further improved by forbidding the "Cooper-pair back-tunneling" in the simulation, which is shown in the lower set of curves.

Fig. 3(b) shows the situation for a dataset with decreaced E_C. The topmost set consists of analytic curves, where at $V_C \lesssim 2V_Q \approx 270$ μV approximation of Eqs. (6) and (7) and at $V_C \gtrsim 2V_Q$ approximation of Eqs. (8) and (9) is used. The two lower sets are simulated at $T = 20$ mK and $T = 300$ mK. Although again qualitatively similar, at $T = 20$ mK the main source of disagreement is the enhancement of $\Gamma_\uparrow$ at a finite temperature. At $T = 300$ mK the spike is spread, since at relatively large temperatures (now $E_C/kT \approx 2.6$) also $\Gamma_\downarrow$ is increased due to incoherent Cooper pair tunneling in a same sense as indicated in Ref.[4].

Fig. 4 shows a comparison of experimental (see Refs.[3] and[5] for detalis) and calculated IV curves. The experiment (Fig. 4(a)) was performed with a current biased base electrode, and the characteristic curves have also been solved for constant I_B in Fig. 4(b). The calculated data is discontinuous at $V_C = 2V_Q$, due to the different dynamics of downward transitions

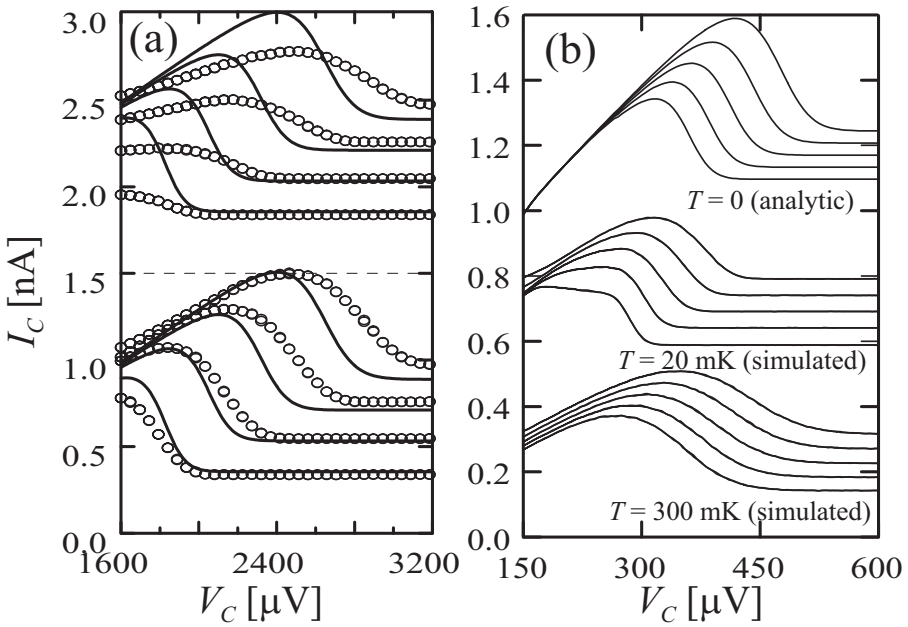

FIG. 3: *(a) Computed $I_C - V_C$ plots for a device otherwise similar to that of Fig. 3 except $R_T = 375$ kΩ, $E_J/E_C = 0.2$ and $\Delta = 0$ (an NIN base junction). The base voltages are $V_B' = -1.0e/C$, -1.5e/C, -2.0e/C, -2.5e/C from down to top (open circles) . Analytic IV curves (solid lines) are calculated from (1) together with approximations from Eqs. (8) and (9). The upper set (lifted by 1.5 nA for clarity) shows the result with the full simulation model, while the lower set shows the result without "Cooper pair back-tunneling". (b) Analytic and computed $I_C - V_C$ plots for a device having $R = 500$ kΩ, $C = 1.2$ fF, $R_T = 250$ kΩ, $\Delta = 200$ μV and $E_J/E_C = 0.3$. The two topmost sets have been lifted by 0.5 nA and 0.8 nA for clarity.*

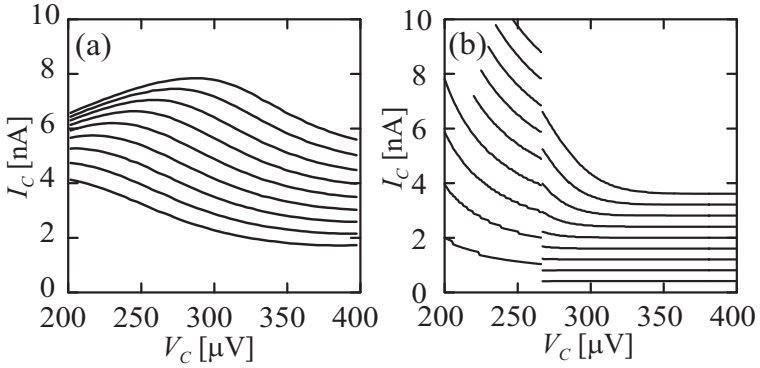

FIG. 4: *Comparison of (a) experimental[5] and (b) calculated data. The parameters are* $R \approx 23$ *kΩ,* $C \approx 1.2$ *fF* $R_T \approx 27.3$ *kΩ and* $E_J/E_C = 0.7$. *The base current is varied from -3.6 nA to -0.4 nA from up to down.*

as explained in Section II. The experimental data is not quite in the validity range of the theory, mainly due to the small value of $R \approx 23$ kΩ. Now $R/R_Q \approx 0.4 E_C/k_B$. Thus the experimental data is partially washed out by fluctuations not included in the theory.

IV. LINEARIZED MODEL AND AMPLIFIER PROPERTIES

To analyze the BOT as an amplifier, we next linearize the model around a point of operation. The linearization is formally given as

$$\begin{bmatrix} i_C \\ i_B \end{bmatrix} = \begin{bmatrix} G_{out} & g_m \\ g_x & G_{in} \end{bmatrix} \begin{bmatrix} v_C \\ v_B \end{bmatrix}, \tag{10}$$

where i_C, i_B, v_C, v_B are the small-signal components of collector and base currents and voltages, i.e. small variations around the point of operation. The definitions of small-signal parameters are $G_{in} = (\partial I_B/\partial V_B)_{V_C}$, $g_m = (\partial I_C/\partial V_B)_{V_C}$, $g_x = (\partial I_B/\partial V_C)_{V_B}$ and $G_{out} = (\partial I_C/\partial V_C)_{V_B}$. By using the definitions and Eqs. (1) and (2) one now obtains the small-signal responce as function of device and bias parameters. Note that V_B is kept constant in the last two partial derivations. This is the natural choice, if the circuit shown in Fig. 1(a) is used. However, if the emitter is voltage biased instead of the collector, V_B' should be fixed instead. The choice does not have an effect on the analysis below, since we will be assuming small R_L, whence V_C is constant (see Fig. 1(a). This renders g_x and G_{out} redundant. In other words, we assume here that the BOT is read out with a current amplifier.

For some purposes it is also useful to define the current gain. $\beta = -(\partial I_C/\partial I_B)_{V_C} = -g_m/G_{in}$. By evaluating g_m and G_{in} from the definitions, this is given as

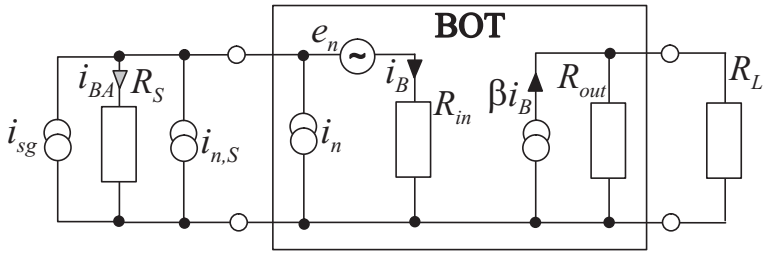

FIG. 5: *A graphical representation of the small signal model of the BOT in the limit of small R_L. The noise added by the BOT is represented with equivalent noise sources i_n end e_n.*

$$\beta = \frac{1}{e}\frac{I_S}{\Gamma_\uparrow \langle N_e \rangle (1-\beta_B)} + 1. \tag{11}$$

Here we have defined

$$\beta_B = -\frac{\Gamma_\downarrow (\Gamma_\uparrow + \Gamma_\downarrow)}{\Gamma_\uparrow \langle N_e \rangle} \left(\frac{\partial \langle N_e \rangle}{\partial V_B} / \frac{\partial \Gamma_\downarrow}{\partial V_B} \right) \tag{12}$$

In the approximation of Eq. (6) β_B is zero, since $\langle N_e \rangle$ is constant. Using Eqs. (8) and (9) instead makes values $\beta_B \approx 1$ possible. We call β_B the "hysteresis parameter" of the BOT.

The noise model for the BOT in the limit of small R_L is shown in Fig. 5. The signal and the noise from the source are described as current generators i_{sg} and $i_{n,S}$ in parallel with the source resistance R_S. The input and output impedances are $R_{in} = 1/G_{in}$ and $R_{out} = 1/G_{out}$. The current generator βi_B at the output accounts for the gain. The noise added by the BOT is represented in a standard fashion (see e.g.[13]) by equivalent voltage and current noise generators (e_n and i_n, respectively) at the input. According to Fig. 5 the output noise of the BOT excluding the contribution of the source ($i_{n,S} = 0$) at the output is

$$S_{i,out}^{1/2} = \frac{1}{R_{in} + R_S} \beta S_{en}^{1/2} + \frac{1/R_{in}}{1/R_{in} + 1/R_S} \beta S_{in}^{1/2}, \tag{13}$$

where S_{en} and S_{in} are the spectral density functions corresponding to e_n and i_n, respectively. Note that e_n and i_n and are fully correlated with equal phases in our model. We next choose

$$S_{en}^{1/2} = \frac{2I_S}{-g_m} \sqrt{\frac{\Gamma_\downarrow \Gamma_\uparrow}{(\Gamma_\uparrow + \Gamma_\downarrow)^3}} \tag{14}$$

$$S_{in}^{1/2} = \frac{2I_S}{\beta} \sqrt{\frac{\Gamma_\downarrow \Gamma_\uparrow}{(\Gamma_\uparrow + \Gamma_\downarrow)^3}}. \tag{15}$$

Physically, the noise current at the output of the BOT $S_{i,out}$ is obtained by assuming that the dominant noise mechanism is the two-level switching noise due to collector current switching between values $I_C \approx 0$ and $I_C = I_S$. It can be shown, that with selections of Eqs. (14)

and (15), Eq. (13) produces the output noise in accordance to the theory of a two-level fluctuator(see e.g.[12]). Furthermore, the generators are independent of R_S. However, the backaction noise (i.e. the noise current i_{BA} through or voltage accross R_S) is not correctly predicted by the model.

The noise figure, defined as the ratio of total noise at the output divided by the noise contributed by the BOT, is $F = 1 + S_{i,out}\left[(\beta R_S)^2 (R_{in} + R_S)^2 S_{in,S}\right]^{-1}$, where $S_{in,S} = 4kT_0/R_S$ is the spectal density function of $i_{n,S}$ and T_0 is a reference temperature. One gets optimum impedance R_{opt} and corresponding minimum noise temperature T_n by minimizing F with respect to R_S and using the definiton $F = 1 + T_n/T_0$. It follows

$$R_{opt} = \sqrt{\frac{S_{en}}{S_{in}}} = |R_{in}| \tag{16}$$

$$T_n = \frac{1}{k_B}\sqrt{S_{en}S_{in}} = \frac{|R_{in}|\, S_{in}}{k_B}. \tag{17}$$

The correlation of the two sources shows in Eq. (17) in such a way that the prefactor is $1/k_B$ instead of $1/2k_B$, which is the case for uncorrelated sources. The difference stems from the fact that now the amplitudes of the two sources rather than the powers are summed.

If the approximation of Eqs. (6) and (7) is used to evaluate $\langle N_e\rangle$ and $\Gamma_\downarrow$ (whence also $\beta_B = 0$), one gets for some gain and noise parameters

$$\beta = 2\langle N\rangle + 1 \tag{18}$$

$$S_{in}^{1/2} = \sqrt{-\frac{4e}{R_T}\left(V_B' + \frac{V_Q}{2}\right)\left(1 + \frac{\Gamma_\downarrow}{\Gamma_\uparrow}\right)^{-3}} \tag{19}$$

$$R_{opt} = R_T\left(1 + \Gamma_\downarrow/\Gamma_\uparrow\right)^2 \tag{20}$$

$$T_n = -\frac{4e}{k_B}\left(V_B' + \frac{V_Q}{2}\right)\left(1 + \frac{\Gamma_\downarrow}{\Gamma_\uparrow}\right)^{-1}. \tag{21}$$

In this mode the BOT acts as a simple "charge multiplier", where one electron trigs $\langle N\rangle$ Cooper pairs, thus $\beta = 2\langle N\rangle + 1$. The current noise can also be expressed as $S_{in}^{1/2} = 2\sqrt{eI_B}\left(1 + \Gamma_\downarrow/\Gamma_\uparrow\right)^{-1}$. In the limit of small $\Gamma_\downarrow/\Gamma_\uparrow$ the Bloch oscillation sequences are short compared the total length of the "duty cycle" $1/\Gamma_\downarrow + 1/\Gamma_\uparrow$. Then the equivalent current noise can be understood to be simply the shot noise of the input current. In that case $S_{in}^{1/2} = 2\sqrt{eI_B}$. The prefactor 2 instead of more familiar $\sqrt{2}$ is due to the random length of charge pulses as opposed to the standard shot noise. With large $\Gamma_\downarrow/\Gamma_\uparrow$, or with long Cooper pair sequences, the noise drops. The impedance also increases because single electron tunneling is forbidden during the Bloch oscillations. One should remember, however, that this is strictly true only in the absence of base junction leakage current.

As noted above, the spectral noise density of the backaction noise current (i_{BA} in Fig. 5) in general differs from $S_{i,in}$. It can be shown, that for either $\Gamma_\uparrow/\Gamma_\downarrow \ll 1$ or $\Gamma_\uparrow/\Gamma_\downarrow \gg 1$, it is exactly that of the base current shot noise, i.e. $\sqrt{2eI_B}$. The maximum suppression of i_{BA} occurs at $\Gamma_\uparrow = \Gamma_\downarrow$, where the fano factor is 1/2. The reason for the difference in the equivalent current noise and the backaction noise is, that in the limit of large $\Gamma_\downarrow/\Gamma_\uparrow$ the output current noise becomes fully anticorrelated with i_{BA}. Thus i_{BA} does not directly determine the current resolution, or vice versa. To minimize the backaction noise, the device should be operated at a low base current. The low limit is here is set by spontaneous downwards transitions due to incoherent Cooper pair tunneling[4].

If the approximation from Eqs. (8) and (9) is used instead of Eqs. (6) and (7) for calculating $\Gamma_\downarrow$ and $\langle N_e \rangle$, the dominating terms are in many cases those dependent on β_B especially if $\beta_B \approx 1$. Here we give estimates of some gain and noise parameters. The derivation details and other parameters are shown in Ref.[11]. The hysteresis parameter is

$$\beta_B = 0.02 \left(\frac{R}{R_T}\right)^2 \exp\left(\frac{\pi e^2 R}{16\hbar}\left(\frac{E_J}{E_c}\right)^2\right), \tag{22}$$

while some other quantities of interest are

$$\beta \approx 1.2\,(1-\beta_B)^{-1} \tag{23}$$

$$S_{in}^{1/2} \approx \frac{12e}{\sqrt{RC}}\left(\frac{R_T}{R}\right)\beta^{-1} \tag{24}$$

$$R_{opt} \approx \frac{R}{2}\beta \tag{25}$$

$$T_n \approx \frac{50E_C}{k_B}\left(\frac{R_T}{R}\right)^2\beta^{-1} \tag{26}$$

As $\beta_B \to 1$ the current gain β diverges. However, the trade-off is that the optimum impedance R_{opt} also diverges. The fluctuation at the output does not depend on β_B, so the current noise $S_{in}^{1/2}$ and the noise temperature T_n decrease at the same time.

The physics in this limit can be understood as follows. With very large β_B the main effect of increasing V_B is increasing the number of electrons $\langle N_e \rangle$ needed to cause a downwards transition (see Eq. 12). This leads to decreasing I_B, i.e. negative input conductance. With very small β_B the only effect of increasing V_B is decreasing $\Gamma_\downarrow$. This leads to increasing I_B, i.e. positive input conductance[14]. At intermediate values, i.e. $\beta_B \approx 1$, the input conductance is close to zero. The effect is that a small change in I_B causes a large change in V_B. Consequently $\Gamma_\downarrow$, and thus also I_C change considerably. This leads to the enhancement of the current gain. Since the noise at the output is not enhanced comparably, this leads to decrease of the equivalent current noise and the noise temperature.

A set of simulated $I_C - I_B$ and $I_B - V_B$-plots with a varying Josephson coupling are shown in Figs. 6(a) and (b). The parameters were chosen so that the device is realizable

with Al-tunnel junctions (see the Caption of Fig. 6). Current biased base electrode was assumed. This shows how the current gain and the input impedance increase without limit, as β_B approaches unity. As β_B exceeds unity the curves become hysteretic. If the source resistance R_S is large, hysteresis is a manifestation of negative input conductance. Therefore a sufficient stability criterion for all source resistances is $\beta_B < 1$. For small source resistances the device is stable independently of β_B. The simulated IV curves become hysteretic at $E_J/E_C \approx 0.25$. According to Eq. (22) $E_J/E_C \approx 0.32$ leads to $\beta_B = 1$. It is also worthwhile to compare the stability criterion to experiments. In Ref.[5] the two samples have $\beta_B \approx 0.07$ and $\beta_B \approx 1500$ according to Eq. (22). The first one does not show hysteresis, whereas the second one does.

The current noise and the minimum noise temperature are shown as the function of the optimum resistance in Fig. 6(c) and (d). The computational noise data was obtained by performing a Fast Fourier Transform for the output current and averaging the low-frequency part. This together with computed small signal paramters gives the equivalent noise parameters. A correct form of dependencies, i.e. $S_{in}^{1/2} \propto R_{opt}^{-1}$ and $T_n \propto R_{opt}^{-1}$ are correctly reproduced as compared to Eqs. (24) - (26). Differences in absolute levels can partially be explained through the inaccuracy of the approximation. To some extent the differences can also be understood with reference to excess noise mechanisms discussed in Section V. However, correct forms of dependencies and the order of magnitude are correctly predicted by the theory.

V. SUMMARY AND DISCUSSION

We have developed an analytic of the BOT based on a two-level system. The two-level picture has some limitations. It excludes the effect of additional noise due to the finite band width of Bloch oscillations with finite R or T. It also excludes the additional noise of the leakage current (due to intraband transitions) through the collector resistance. Also the evaluation of transition rates at the limit of low T and large R introduces some error. The agreement with finite temperature data was, however, generally good suggesting that the approach is sufficient to yield quantitative predictions in the limit under discussion. Expressions for amplifier properties such as gain, stability, impedance levels and noise parameters were derived enabling amplifier optimization for a given purpose. It was shown that equivalent current noise spectral densities below 1 fA/$\sqrt{\text{Hz}}$ and noise levels below 0.1 K can be obtained with optimum impedance levels of order a few MΩ. According to finite-temperature simulations the noise temperature of the BOT can also be brought below its physical temperature.

Most other well-known mesoscopic amplifiers, e.g. single-electron transistor (SET)[15] or single Cooper pair transistor (SCPT)[16] are based on controlling a current flow by charging a gate electrode. The BOT is, on the other hand based on controlling the state of a JJ

by means of quasiparticle tunneling events. This makes it insensitive to bakcground charge fluctuations, whence 1/f noise is smaller. This makes it potentially better in low-frequency applications.

BOT was generally found to work in two modes. The first one is a simple quasiparticle - $\langle N \rangle$ Cooper pair converter. In the second mode intraband transitions play a role. These can be utilized to enhance amplification and suppress equivalent noise, but make the device potentially unstable. A stability criterion was derived and quantified by the hysteresis

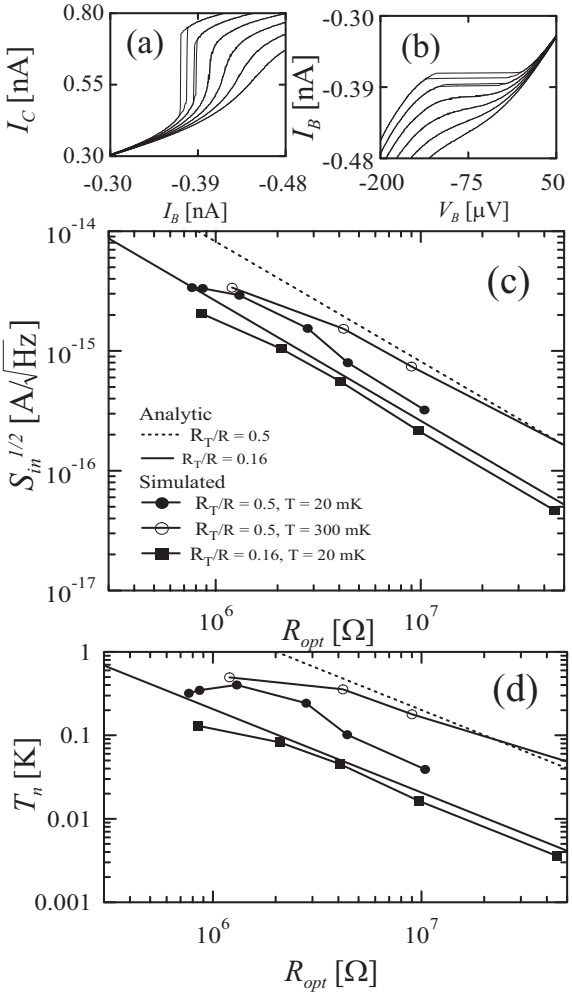

FIG. 6: *(a) and (b) Computed $I_C - V_C$ and $I_B - V_B$ curves ($R = 500\ k\Omega$, $C = 1.2\ fF$, $\Delta = 200\ \mu V$, $T = 20\ mK$ and $R_T/R = 0.5$) The Josephson coupling E_J/E_C is varied from 0.18 to 0.28 (from left to right in (a) and down to up in (b)). (c) The current noise spectral density S_{in} referred to input and (d) the minimum noise temperature T_n as function of R_{opt}. Within each dataset E_J/E_C (or equivalently β_B) is varied. In (c) and (d) the parameters are as above with the exceptions of varying R_T/R and T as shown in the legend. The bias point in the simulations with $T = 20\ mK$ is $V_C = 3.5e/C$ and $V_C = 4.5e/C$ for those with $T = 300\ mK$.*

parameter β_B.

Authors wish to acknowledge J. Delahaye, P. Hakonen and R. Lindell for their contribution. The work was supported by the Academy of Finland (project 103948).

---

[1] H. Seppä, and J. Hassel, cond-mat/0305263 (2003).

[2] J. Hassel, and H. Seppä. IEEE Trans. Appl. Supercond 11, 260 (2001).

[3] J. Delahaye, J. Hassel, R. Lindell, M. Sillanpää, M. Paalanen, H. Seppä, and P. Hakonen, Science 299, 1045 (2003).

[4] J. Delahaye, J. Hassel, R. Lindell, M. Sillanpää, M. Paalanen, H. Seppä, and P. Hakonen, Phys. E 18, 15 (2003).

[5] J. Hassel, J. Delahaye, H. Seppä, and P. Hakonen, J. Appl. Phys. 95, 8059 (2004).

[6] K.K. Likharev and A.B. Zorin, J. Low Temp. Phys. 59, 348 (1985).

[7] G. Schön, A.D. Zaikin, Phys. Rep. 198, 237 (1990).

[8] M.H. Devoret, D. Esteve, H. Grabert, G.-L. Ingold, H. Pothier and C. Urbina, Phys. Rev. Lett. 64, 1824 (1990).

[9] G.-L. Ingold and Yu. V. Nazarov, in Single Charge Tunneling, edited by H. Grabert and M.H. Devoret (Plenum Press, New York 1992), pp. 21-106.

[10] A.D. Zaikin and D.S. Golubev, Phys. Lett. A 164, 337 (1992).

[11] Derivation details, submitted to Electronic Auxillary Publications Service (EPAPS) (2004).

[12] Sh. Kogan, Electronic Noise and Fluctuations in Solids (Cambridge University Press 1996).

[13] J. Engberg, and T. Larsen, Noise Theory of Linear and Nonlinear Circuits (John Wiley & Sons 1995).

[14] Note that with our sign conventions ($V_B < 0$, $I_B < 0$) electrons are tunneling to the island, i.e. Increasing V_B decreases $\Gamma_\downarrow$, which increases I_B. On the other hand, increasing V_B increases $\langle N_e \rangle$, which decreases I_B.

[15] D. Averin, and K.K Likharev, J. Low Temp. Phys. 62, 345 (1986).

[16] A.B. Zorin, Phys. Rev. Lett. 76, 4408 (1996).

[17] F.N.H. Robinson, Noise and Fluctuations in electronic devices and circuits, Oxford university press (1974).

Theory of the Bloch Oscillating Transistor: Derivation details

Appendix A: Downwards tunneling probabilities

To calculate $\langle N_e \rangle$ and $\Gamma_\downarrow$ we first derive an approximation for the quasiparticle tunneling rate through the base junction as function of charge $\Gamma_{QP1}(Q)$. Neglecting the thermal rounding we get

$$\Gamma_{QP1}(t) = \frac{1}{R_T C}\left(\frac{V_1}{V_Q} - \frac{1}{2}\right) \quad (1)$$
$$= \frac{1}{R_T C}\left(\frac{Q(t)}{e} - \frac{V_C + V_B'}{V_Q} - \frac{1}{2}\right), \text{ if } |V_1| > V_G$$
$$\Gamma_{QP1}(t) = 0, \text{ if } |V_1| < V_G,$$

where the gap-voltage is V_G, i.e., we neglect the leakage current at the subgap voltages. In the most straightforward experimental realization the base junction is a NIS junction. In this case $V_G = \Delta + V_Q/2$ including the contribution of both superconducting and Coulomb gaps. In principle it is also possible to realize the base junction as a NIN junction, i.e. with suppressed superconductivity on the other electrode. Then the gap voltage is $V_G = V_Q/2$. In general, Γ_{QP1} is a function of time due to the time dependency of charge.

We next separate two different regimes to find analytic approximations for $\langle N_e \rangle$ and $\Gamma_\downarrow$. If $V_C < 2V_Q$ one electron always suffices to return the system to the first level, i.e., $\langle N_e \rangle = 1$. In this case the probability distribution of the first quasiparticle tunneling event after the Zener tunneling is

$$P(t) = \Gamma_{QP1}(t) \lim_{\Delta t \to 0} \prod_{j=1}^{t/\Delta t} \left(1 - \Gamma_{QP1}(j\Delta t)\right), \quad (2)$$

which is the probability that an electron will tunnel at time t times the probability that it has not tunneled at earlier times. The charge in Eq. (1) before the first quasiparticle event obeys simple RC-relaxation, i.e.

$$Q(t) = CV_C\left(1 + \left(\frac{V_Q}{V_C} - 1\right)e^{-\frac{1}{RC}t}\right), \quad (3)$$

where we assumed that Zener tunneling occurs at $t = 0$ (or equivalently that $Q(0) = e$). The average rate $\Gamma_\downarrow$ is the inverse of the weight of the distribution given by Eq. (2). Thus

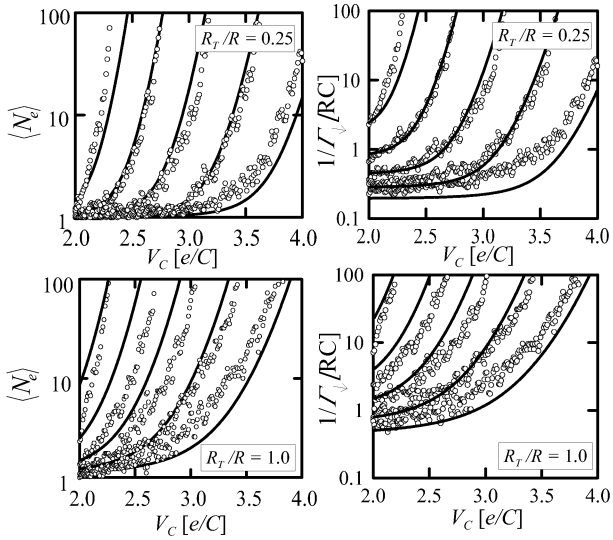

FIG. 1: Computed data for $\langle N_e \rangle$ and $\Gamma_\downarrow$ obtained by solving Eqs. (1) and (3) numerically (open circles). In each frame the base voltage is varied as $V_B' = -1.0e/C$, -1.5e/C, -2.0e/C, -2.5e/C, -3.0e/C from left to right. The lines correspond the fits, i.e. Eqs. (7) and (8).

$$\langle N_e \rangle = 1 \quad (4)$$
$$\Gamma_\downarrow = \frac{1}{\int_0^\infty tP(t)\,dt}. \quad (5)$$

In general, the downwards rate has to be evaluated numerically from (5). However, if we further assume that the transient in Eq. (3) is short, Eq. (2) reduces to a simple exponential distribution. This is equivalent to assuming that $Q(t) \approx CV_C$ at all times, and thus Eq. (1) also becomes time independent. Now simply $\Gamma_\downarrow = \Gamma_{QP1}$, and it follows

$$\Gamma_\downarrow = -\frac{1}{CR_T}\left(\frac{V_B'}{V_Q} + \frac{1}{2}\right). \quad (6)$$

If $V_C > 2V_Q$ it is possible that the first electron tunneling through the base junction does not cause a transition to the first level, but some of the single quasiparticle events lead to intralevel transitions instead. To solve $\langle N_e \rangle$ and $\Gamma_\downarrow$ analytically from Eqs. (1) and (3) in this

case is unfortunately impossible. To find a sufficient approximation for our purposes, we have solved the problem numerically and searched for a proper fitting function. For simplicity we have assumed an NIN junction at the base electrode, i.e. $V_G = V_Q/2$ in Eq. (1). Some fits are shown in Fig. 1 and the result is

$$\langle N_e \rangle = 0.04 \left(\frac{R_T}{R}\right)^2 \times \exp\left(0.3 \exp\left(1.8\frac{V_C}{V_Q} + 0.27\frac{V_C V_B'}{V_Q^2} - 0.2\frac{V_B'}{V_Q}\right)\right) + 1 \tag{7}$$

$$\Gamma_\downarrow^{-1} = -\left(\frac{\partial I_C}{\partial I_B}\right)_{V_C} = 1.2e\frac{R+R_T}{V_B'}\left(1 - \langle N_e \rangle\right) + RC\left(2.5\frac{R_T}{R} + 1.1\right)\left(\frac{V_Q}{V_B'}\right)^2. \tag{8}$$

Appendix B: Hysteresis and noise parameters

In this Appendix we show the derivation of hysteresis and noise parameters in the limit $\beta_B \approx 1$. The starting points are the definitions

$$\beta_B = -\frac{\Gamma_\downarrow\left(\Gamma_\uparrow + \Gamma_\downarrow\right)}{\Gamma_\uparrow \langle N_e \rangle}\left(\frac{\partial \langle N_e \rangle}{\partial V_B} / \frac{\partial \Gamma_\downarrow}{\partial V_B}\right) \tag{9}$$

$$g_m = I_S \frac{\Gamma_\uparrow}{\left(\Gamma_\uparrow + \Gamma_\downarrow\right)^2}\frac{\partial \Gamma_\downarrow}{\partial V_B} + G_{in} \tag{10}$$

$$\beta = \frac{1}{e}\frac{I_S}{\Gamma_\uparrow \langle N_e \rangle \left(1 - \beta_B\right)} + 1 \tag{11}$$

$$S_{en}^{1/2} = \frac{2I_S}{-g_m}\sqrt{\frac{\Gamma_\downarrow \Gamma_\uparrow}{\left(\Gamma_\uparrow + \Gamma_\downarrow\right)^3}} \tag{12}$$

$$S_{in}^{1/2} = \frac{2I_S}{\beta}\sqrt{\frac{\Gamma_\downarrow \Gamma_\uparrow}{\left(\Gamma_\uparrow + \Gamma_\downarrow\right)^3}}, \tag{13}$$

$$R_{opt} = \sqrt{\frac{S_{en}}{S_{in}}} \tag{14}$$

$$T_n = \frac{1}{k_B}\sqrt{S_{en} S_{in}}. \tag{15}$$

The main task is to get sufficient estimates for I_S, $\Gamma_\downarrow$, $\Gamma_\uparrow$, $\langle N_e \rangle$, $\partial \langle N_e \rangle / \partial V_B$ and $\partial \Gamma_\downarrow / \partial V_B$ near an interesting point of operation. We note that for the approximation from Eqs. (7) and (8) used for $\langle N_e \rangle$ and $\Gamma_\downarrow$ to apply the collector voltage must satisfy $V_C \gtrsim 2V_Q$. For simplicity we assume that $V_C = 2V_Q$. When the system is at the second level, the voltage across the JJ is $V_2 \gtrsim V_Q$ and the collector current consists of the leakage current only, i.e. $I_C = -I_B$. Assuming that $V_2 = V_Q$ and that the base junction roughly acts as a linear resistor we get by analyzing the circuit of Fig. 1(a) and noting that by definition $V_B = V_B' + V_C$ the result $V_B' = -V_Q\left(1 + R_T/R\right)$, i.e. we have found estimates for the bias parameters. Using these and Eqs. (**??**), (**??**) and (7) we can readily write:

$$I_S \approx \frac{2e}{RC\ln 3} \tag{16}$$

$$\Gamma_\uparrow \approx \frac{1}{RC\ln 3}\exp\left(-\frac{\pi RC}{8\hbar}\frac{E_J^2}{E_c^2}E_C\right) \tag{17}$$

$$\langle N_e \rangle \approx 100\left(\frac{R_T}{R}\right)^2. \tag{18}$$

In the last Equation we have also utilized the assumption $R_T \lesssim R$.

To find an estimate for $\Gamma_\downarrow$ we can use physical intuition and insight learned from simulations. Since the operation is based on switching between the two states, the system spends roughly as much time in both states. Thus

$$\Gamma_\downarrow \approx \Gamma_\uparrow. \tag{19}$$

Although some error may be introduced by doing this, it is not too severe, since most properties depend more strongly on the derivative $\partial \Gamma_\downarrow / \partial V_B$, which will be calculated separately.

The derivative $\partial \langle N_e \rangle / \partial V_B$ is obtained by direct differentiation of Eq. (7), inserting the bias parameters V_B, V_C from above and applying the approximation $R_T \lesssim R$:

$$\frac{\partial \langle N_e \rangle}{\partial V_B} \approx \frac{270}{V_Q}\left(\frac{R_T}{R}\right)^2. \tag{20}$$

To obtain $\partial \Gamma_\downarrow / \partial V_B$ we first note that $\Gamma_\downarrow$ depends on V_B both through the explicit dependence in Eq. (8) and through $\langle N_e \rangle$. Since $\langle N_e \rangle$ depends very strongly on V_B we will approximate $\partial \Gamma_\downarrow / \partial V_B \approx \left(\partial \Gamma_\downarrow / \partial \langle N_e \rangle\right)\left(\partial \langle N_e \rangle / \partial V_B\right)$. By differentiation of Eq. (8), application of the bias parameters V_B and V_C from above and using Eq. (20) we get

$$\frac{\partial \Gamma_\downarrow}{\partial V_B} \approx 1.2e\Gamma_\downarrow^2 \frac{R+R_T}{V_B'}\frac{\partial \langle N_e \rangle}{\partial V_B}.$$

By using Eqs. (19) and (17) we now get

$$\frac{\partial \Gamma_\downarrow}{\partial V_B} \approx -\frac{290}{V_Q}\frac{1}{RC}\left(\frac{R_T}{R}\right)^2\left(\exp\left(-\frac{\pi RC}{8\hbar}\frac{E_J^2}{E_c^2}E_C\right)\right)^2. \tag{21}$$

By inserting Eqs. (16)-(21) into Eq. (9) we get the estimate

$$\beta_B = 0.02\left(\frac{R}{R_T}\right)^2 \exp\left(\frac{\pi e^2 R}{16\hbar}\left(\frac{E_J}{E_c}\right)^2\right), \tag{22}$$

The exponent (or $\langle N \rangle$) in Eqs. (17) and (21) affects on the device parameters mainly through β_B. For other purposes we may assume it roughly constant and solve it by setting $\beta_B = 1$ in Eq. (22), whence Eqs. (17) and (21) are simplified into

$$\Gamma_\uparrow \approx \frac{0.015}{RC}\left(\frac{R}{R_T}\right)^2 \tag{23}$$

$$\frac{\partial \Gamma_\downarrow}{\partial V_B} \approx -\frac{0.08}{V_Q}\frac{1}{RC}\left(\frac{R}{R_T}\right)^2. \tag{24}$$

The results

$$\beta \approx 1.2\,(1-\beta_B)^{-1} \tag{25}$$

$$g_m \approx -\frac{2}{R} \tag{26}$$

$$S_{in}^{1/2} \approx \frac{12e}{\sqrt{RC}}\left(\frac{R_T}{R}\right)\beta^{-1} \tag{27}$$

$$S_{en}^{1/2} \approx \frac{2e}{\sqrt{RC}}R_T \tag{28}$$

$$R_{opt} \approx \frac{R}{2}\beta \tag{29}$$

$$T_n \approx \frac{50E_C}{k_B}\left(\frac{R_T}{R}\right)^2\beta^{-1} \tag{30}$$

now follow by inserting Eqs. (16), (18), (19), (20), (23) and (24) into the definitions of interesting quantities, i.e. Eqs. (10), (11), (12), (13), (14) and (15).